RSC Advances

PAPER

View Article Online
View Journal | View Issue

Cite this: *RSC Adv.*, 2022, **12**, 14450

Catalytic oxygen evolution from hydrogen peroxide by *trans*-$[Co(en)_2Cl_2]$@InBTB metal–organic framework catalytic system†

Sukbin Yoon,[a] In-Hwan Choi,[a] Youngmee Kim *[b] and Seong Huh *[a]

Received 5th April 2022
Accepted 6th May 2022

DOI: 10.1039/d2ra02208g

rsc.li/rsc-advances

The diethylammonium counter-cations of the $[Et_2NH_2]_3[In_3(BTB)_4]$ metal–organic framework (InBTB MOF, BTB = 1,3,5-benzenetribenzoate) with an anionic framework can be effectively exchanged with cationic *trans*-$[Co(en)_2Cl_2]^+$ complex ions through a simple cation-exchange process. The heterogenized *trans*-$[Co(en)_2Cl_2]^+$-encapsulated InBTB MOF (*trans*-$[Co(en)_2Cl_2]$@InBTB) catalytic system maintained the activity of the captured *trans*-$[Co(en)_2Cl_2]^+$ complex ion for hydrogen peroxide decomposition in aqueous solution under mild reaction conditions. The captured *trans*-$[Co(en)_2Cl_2]^+$ complex also exhibited *trans*–*cis* isomerization to produce either *cis*-$[Co(en)_2Cl_2]$@InBTB or *cis*-$[Co(en)_2(H_2O)Cl]$@InBTB based on IR spectroscopic investigation. The *trans*-$[Co(en)_2Cl_2]$@InBTB catalytic system showed high recyclability for oxygen evolution from hydrogen peroxide. The catalytic ability of *trans*-$[Co(en)_2Cl_2]$@InBTB was maintained up to seven times of recycling.

1. Introduction

The large channels present in metal–organic frameworks (MOFs) are ideal hosts for encapsulating various functional guests including catalytically active transition metal complexes,[1,2] viologens,[3] optical dyes,[4–11] metallic nanoparticles,[12–15] and drug molecules.[16,17] The crystalline nature of the frameworks and channels provide highly ordered spatial arrangements of the encapsulated guests compared to other porous materials. The catalytic activities of captured guests can be efficiently preserved or enhanced and the optical activities of the dye guests can be systematically controlled through simple encapsulation into channels of MOFs. In particular, MOFs with negatively charged frameworks contain counter-cations in the channels. Negative framework charges often develop due to the charge unbalance between cationic metal ions and anionic bridging ligands. The counter-cations near the metal centres counterbalance the charge mismatch to satisfy charge neutrality. The presence of these counter-cations and anionic frameworks often renders MOFs more functional. For example, the counter-cations can be readily replaced with other functional cationic guests through a simple cation-exchange process. Several excellent examples of this process for the preparation of functional MOF systems have recently been reported.[1–6]

A large cationic Reichardt's dye (RD) could be effectively encapsulated into the mesoscale channels of three-dimensional (3D) InBTB MOF ($[Et_2NH_2]_3[In_3(BTB)_4]\cdot 10DEF\cdot 14H_2O$, H_3BTB = 1,3,5-benzenetribenzoic acid, DEF = *N*,*N*-diethylformamide) through cation-exchange to give RD@InBTB.[4] The doubly interpenetrated framework structure of InBTB is shown in Fig. S1† (ESI). A partially encapsulated RD exhibited a quite distinct absorption behaviour compared to free RD crystals due to confinement effects. Similarly, organic dipolar chromophore, 4-(4-(diphenylamino)styryl)-1-dodecylpyridinium bromide (DPASD), has been orderly encapsulated into another phase of InBTB (= ZJU-28) to afford DPASD@ZJU-28 exhibiting highly active nonlinear optical (NLO) property.[5] Several cationic dyes were also effectively incorporated into InBTB to give a series of dye@InBTB MOFs with good optical properties.[6] These examples clearly suggest that the cation-exchange-driven generation of functional MOFs is a promising strategy to develop new MOF systems with diverse functions.

Additionally, the relatively strong electrostatic interaction between the cationic guests and anionic frameworks is very suited for simple immobilization of catalytically active cationic species inside MOF channels to generate recyclable catalytic systems.[1,2] The encapsulated catalytic species can also be stabilized due to confinement effects. Thus, there are lots of opportunities to prepare recyclable heterogeneous catalytic systems using MOFs with anionic frameworks. In this sense, Rosseinsky *et al.* reported a system in which the catalytically active organometallic cation, $[CpFe(CO)_2(L)]^+$ (Cp = η^5-$C_5H_5^-$, L

[a]*Department of Chemistry and Protein Research Center for Bio-Industry, Hankuk University of Foreign Studies, Yongin 17035, Republic of Korea. E-mail: shuh@hufs.ac.kr; Fax: +82 31 330 4566; Tel: +82 31 330 4522*

[b]*Department of Chemistry and Nano Science, Ewha Womans University, Seoul 120-750, Republic of Korea. E-mail: ymeekim@ewha.ac.kr*

† Electronic supplementary information (ESI) available: Framework structure, PXRD patterns, photo images of crystals, IR spectra, and table of unit cell parameters. See https://doi.org/10.1039/d2ra02208g

= weakly coordinating solvent), was successfully encapsulated into the channels of a 3D anionic InBTC MOF ($[Et_4N]_3[In_3(BTC)_4]$, H_3BTC = 1,3,5-benzenetricarboxylic acid) through cation-exchange process.[1] This approach was employed to develop a series of new functional MOFs for diverse chemical applications.[2,3]

In search of a recyclable heterogeneous O_2 evolution catalytic system, an attempt was made to encapsulate cationic O_2 evolution catalyst into the channels of InBTB. The large mesoscale channels of InBTB allowed the incorporation of a functional cationic Co(III) complex ion, *trans*-$[Co(en)_2Cl_2]^+$ where en is an ethylenediamine,[18] through a simple cation-exchange method as shown in Fig. 1. Although there are two recent articles to review current progress of MOFs encapsulating various dyes and complex ions,[19,20] the catalytic activity and *trans–cis* isomerization of the captured *trans*-$[Co(en)_2Cl_2]^+$ ion in large mesoscale channels of MOF are worth of investigation because *trans–cis* isomerization of the captured cationic complex in nanoscopic space of MOF has not yet been explored.

2. Experimental methods

2.1. Synthesis of InBTB MOF and *trans*-$[Co(en)_2Cl_2]Cl$

The as-prepared InBTB was synthesized according to literature method.[4] *Trans*-$[Co(en)_2Cl_2]Cl$ was prepared according to literature method.[18]

2.2. Encapsulation of *trans*-$[Co(en)_2Cl_2]Cl$ into InBTB MOF

The as-prepared InBTB MOF (10 mg) was added into 2 mM ethanol solution containing *trans*-$[Co(en)_2Cl_2]Cl$ (10 mL). Encapsulation amount was measured by using UV/Vis spectrophotometer every 24 h for 120 h. Each measurement was performed by diluting 500 μL of the aliquot with 500 μL of ethanol in 1 mL quartz cuvette.

2.3. Isomerization reaction of *trans*-$[Co(en)_2Cl_2]Cl$ into *cis*-$[Co(en)_2Cl_2]Cl$ in H_2O

The *trans–cis* isomerization experiment was conducted by following the literature method.[18] The *trans*-$[Co(en)_2Cl_2]Cl$ (0.1 g) was dissolved in 3 mL of deionized water on a watch glass. The aqueous solution was kept at room temperature for 10 min. The watch glass was placed on the top of steam bath. After water was completely evaporated, violet solid product (*cis*-isomer) was formed.

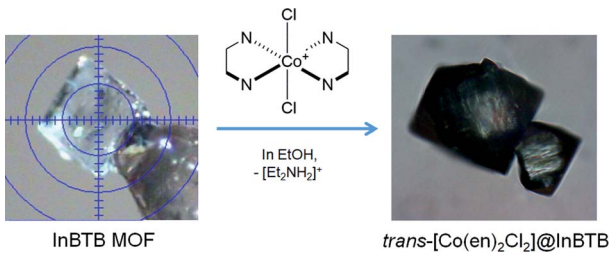

Fig. 1 Schematic of the preparation of *trans*-$[Co(en)_2Cl_2]$@InBTB through the cation-exchange of $[Et_2NH_2]^+$ with *trans*-$[Co(en)_2Cl_2]^+$.

2.4. Isomerization of *trans*-$[Co(en)_2Cl_2]$@InBTB into *cis*-$[Co(en)_2Cl(H_2O)]$@InBTB or *cis*-$[Co(en)_2Cl_2]$@InBTB in H_2O

The *trans*-$[Co(en)_2Cl_2]$@InBTB (5 mg) was transferred into a vial. Deionized water (5 mL) was added into the vial. The vial was sealed with a cap. Isomerization was carried out at 40 °C in water bath. The digital photo images of the sample in the vial were taken every 20 min for 120 h.

2.5. Catalytic decomposition of H_2O_2 by *trans*-$[Co(en)_2Cl_2]$@InBTB

The *trans*-$[Co(en)_2Cl_2]$@InBTB (0.0293 g, 0.0140 mmol based on *trans*-$[Co(en)_2Cl_2]^+$ ion) was transferred into a round bottom vial. Deionized water (20 mL) and 12.18 μL (0.140 mmol) of 34.5% H_2O_2 were added into the vial. The opening of the vial was covered loosely with aluminum foil. The reaction mixture was gently shaken at 40 °C in water bath. Titration was carried out periodically to monitor the decomposition of H_2O_2. Analyte was prepared by diluting 300 μL of aliquot with 22.5 mL of deionized water and acidifying with 79.5 μL of c-H_2SO_4. $KMnO_4$ solution (0.08412 mM) was used as a titrant. After catalytic H_2O_2 decomposition, catalyst was filtered by using a P5-grade glass filter funnel and washed with deionized water. The retrieved catalyst was air-dried overnight and reused for recycling.

2.6. Physical measurements

Powder X-ray diffraction (PXRD) patterns were obtained using a Bruker New D8 Advance diffractometer (40 kV, 40 mA, step size = 0.02°). X-ray photoelectron spectroscopy (XPS) measurement was performed using an ESCA 2000 equipped with Al Kα as an X-ray source. The spectrum was calibrated by using C 1s signal at 284.6 eV. FT-IR spectra in attenuated total reflection (ATR) mode were recorded on a Jasco FT/IR-4100 spectrometer (Jasco, Japan). UV/Vis spectra were recorded on a Scinco S-3100 spectrophotometer (Scinco, Korea).

2.7. Crystallography

The unit cell dimensions of *trans*-$[Co(en)_2Cl_2]$@InBTB was analyzed with a Bruker APEX-II diffractometer equipped with a monochromator using a Mo Kα ($\lambda = 0.71073$ Å) incident beam (CCDC 2142611).

3. Results and discussion

3.1. Preparation of *trans*-$[Co(en)_2Cl_2]$@InBTB

The *trans*-$[Co(en)_2Cl_2]^+$ complex was encapsulated into the channels of the as-prepared InBTB in ethanol solution. The free *trans*-$[Co(en)_2Cl_2]^+$ readily underwent *trans–cis* isomerization in deionized water at room temperature (RT) through aquation (Fig. 2a). The aquation facilitated the dissociation of chloride ligand and subsequent isomerization in water.[21] Contrarily, the *cis*-isomer spontaneously converted back into *trans*-isomer in the ethanol solution. Therefore, *trans*-isomer seemed to be more stabilized in ethanol. Jacewicz *et al.* reported that the conversion of *cis*-$[Co(en)_2Cl_2]^+$ into *trans*-$[Co(en)_2Cl_2]^+$ is a first order reaction in methanol.[22] This process was also strongly

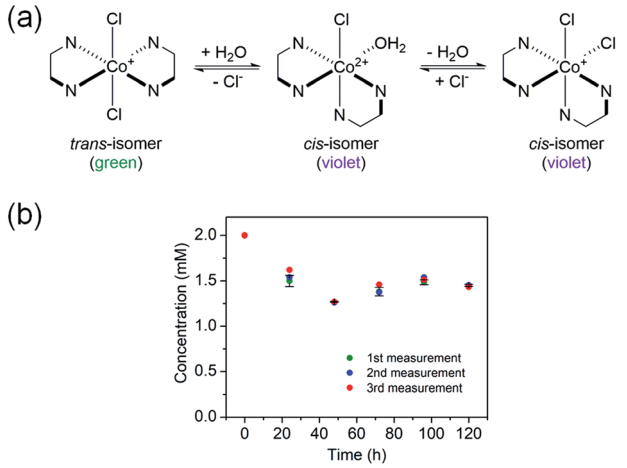

Fig. 2 (a) The *trans–cis* isomerization process of *trans*-$[Co(en)_2Cl_2]^+$ *via* aquation in water. (b) Time courses of the encapsulation of *trans*-$[Co(en)_2Cl_2]^+$ ion by as-prepared InBTB in ethanol. The measurements were performed in triplicate.

solvent dependent and the methanol solvent required high activation barrier. In this case, the dissociation of one of the $-NH_2$ group of the en ligand was a key step for the *trans–cis* isomerization. The *trans*-form (green) and *cis*-form (violet) showed different colors, so the process could be easily monitored by naked eyes and UV/Vis spectroscopy. Thus, ethanol could be chosen as a solvent for the encapsulation of *trans*-$[Co(en)_2Cl_2]^+$ to retard the *trans–cis* isomerization during encapsulation. The encapsulation amount after 5 days of immersion of as-prepared InBTB (10 mg) in 2 mM ethanol solution of *trans*-$[Co(en)_2Cl_2]Cl$ (10 mL) was 5.55 μmol/10 mg-solid (Fig. 2b). The encapsulation amount of the monovalent *trans*-$[Co(en)_2Cl_2]^+$ ion was slightly larger than the values, 3.3–4.2 μmol/10 mg-solid, observed for a series of RuL_3@InBTB MOFs encapsulating divalent cationic $[RuL_3]^{2+}$ polypyridine complexes: $[Ru(bpy)_3]^{2+}$ (bpy = 2,2′-bipyridine), $[Ru(phen)_3]^{2+}$ (phen = 1,10-phenanthroline), and $[Ru(bpz)_3]^{2+}$ (bpz = 2,2′-bipyrazine).[2] This discrepancy was mainly rooted in the smaller ion size of *trans*-$[Co(en)_2Cl_2]^+$ ion than $[RuL_3]^{2+}$ ions.

Although the crystallinity of InBTB was moderately preserved after encapsulation, single crystal analysis of *trans*-$[Co(en)_2Cl_2]$@InBTB was not successfully refined due to disordering of BTB ligand and relatively poor crystal quality compared to as-prepared InBTB. Nonetheless, the observed unit cell dimension change indicated the successful encapsulation of *trans*-$[Co(en)_2Cl_2]^+$ ions. The unit cell dimension of $a = 44.2269(19)$, $b = 44.2269(19)$, $c = 42.519(2)$ Å for InBTB changed into $a = 44.879(8)$, $b = 44.879(8)$, $c = 42.029(7)$ Å for *trans*-$[Co(en)_2Cl_2]$@InBTB. While the trigonal unit cell dimensions of *a*- and *b*-axes for *trans*-$[Co(en)_2Cl_2]$@InBTB slightly increased but that of *c*-axis slightly decreased compared to as-prepared InBTB.[4] The original unit cell dimensions of trigonal cell of InBTB tended to vary depending on the encapsulated guest ions as summarized in Table S1† (ESI). The approximate molecular dimension of *trans*-$[Co(en)_2Cl_2]^+$ ion is $9.90 \times 9.76 \times 8.15$ Å^3. The dimension of the mesoscale channel of InBTB was estimated from the center-to-center distance of two alternating BTB ligands shown in Fig. S1† (ESI). The values are 27.034(1) and 15.486(1) Å.[4] Therefore, the channel of InBTB is large enough to encapsulate *trans*-$[Co(en)_2Cl_2]^+$ ion. It is worth noting that if the size of guest ions were suitable for the encapsulation into the channels, the spatial orientation of them would be more or less predetermined due to the fixed geometry of channels. This implied the possibility that guest ions were likely to be spatially arranged in a controlled manner on demand.

The successful incorporation of *trans*-$[Co(en)_2Cl_2]^+$ ion was also confirmed by X-ray photoelectron spectroscopy (XPS) as shown in Fig. 3. The signals of Co $2p_{3/2}$ and Co $2p_{1/2}$ were observed at 780.73 and 796.11 eV, respectively.[23] The estimated atom% ratio between In and Co elements was 1 : 0.65. The powder X-ray diffraction (PXRD) pattern of *trans*-$[Co(en)_2Cl_2]$@InBTB indicated decreased crystallinity compared to that of as-prepared InBTB (Fig. S2, ESI†). We also observed similar phenomenon when we used EtOH for encapsulation of various cationic dyes.[6] Nonetheless, we believe that the metal–ligand connectivity may not be seriously damaged because *trans*-$[Co(en)_2Cl_2]^+$ ions did not leach out during catalytic reactions.

3.2. *Trans–cis* isomerization of the captured *trans*-$[Co(en)_2Cl_2]^+$ ion of *trans*-$[Co(en)_2Cl_2]$@InBTB

Interestingly, the green color of *trans*-$[Co(en)_2Cl_2]$@InBTB changed very slowly into violet in the solid state over a couple of months. It was speculated that *trans*-isomer slowly isomerized into *cis*-form inside the channels. Although it was unable to identify water molecules in solid-state *trans*-$[Co(en)_2Cl_2]$@InBTB, it seemed that a small amount of water was present inside the channels and the aquation and isomerization slowly occurred in the confined spaces. This observation was quite remarkable because the *trans–cis* isomerization of metal complexes inside MOF channels has not been reported yet. It was believed that the mesoscale channels of InBTB behaved as a nanoscale flask.

To further confirm the *trans–cis* isomerization of the *trans*-$[Co(en)_2Cl_2]^+$ ion, *trans*-$[Co(en)_2Cl_2]^+$ was treated in deionized water at 40 °C and its spectral changes were monitored for 1 h by UV/Vis spectroscopy (Fig. 4a). As expected, the gradual decrease of absorption band at 619 nm for *trans*-$[Co(en)_2Cl_2]^+$ ion and a gradual increase of a new signal at 505 nm for *cis*-

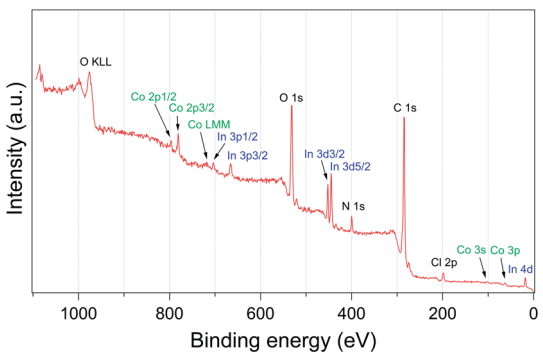

Fig. 3 Survey XPS spectrum of *trans*-$[Co(en)_2Cl_2]$@InBTB.

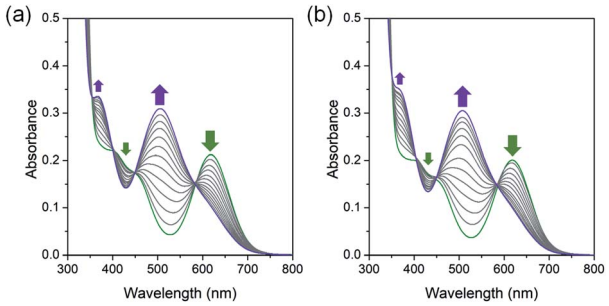

Fig. 4 UV/Vis spectral change during the *trans–cis* isomerization process of *trans*-$[Co(en)_2Cl_2]^+$ ion. (a) *trans*-$[Co(en)_2Cl_2]Cl$ in deionized water at 40 °C for 1 h. (b) *Trans*-$[Co(en)_2Cl_2]Cl$ in deionized water with hydrogen peroxide at 40 °C for 1 h. Green and violet arrows indicate the absorption signals from *trans*-$[Co(en)_2Cl_2]^+$ and *cis*-$[Co(en)_2Cl(H_2O)]^{2+}$ ions, respectively.

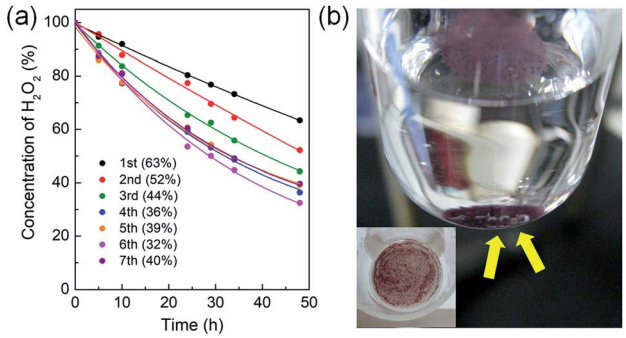

Fig. 5 (a) The conversions of the hydrogen peroxide decomposition catalyzed by *trans*-$[Co(en)_2Cl_2]$@InBTB at 40 °C. The catalyst was recycled up to seven times. (b) The color-changed *trans*-$[Co(en)_2Cl_2]$@InBTB catalyst during the decomposition of hydrogen peroxide. Yellow arrows indicate the oxygen bubbles formed on the surfaces of MOF crystals during the decomposition of hydrogen peroxide. Inset shows violet solids recovered using a glass frit after reaction.

$[Co(en)_2Cl(H_2O)]^{2+}$ ion clearly indicated the instantaneous occurring of the aquation-induced isomerization.[21] Interestingly, once hydrogen peroxide (H_2O_2) was added in the above solution very similar spectral changes were observed (Fig. 4b). Thus, the *trans–cis* isomerization also occurred in the presence of hydrogen peroxide.

3.3. Hydrogen peroxide decomposition by *trans*-$[Co(en)_2Cl_2]$@InBTB

The generation of O_2 from hydrogen peroxide is an important process in biochemistry and water treatment.[24] The catalytic process generating oxygen source from hydrogen peroxide also became increasingly important for partial oxidation of propene to produce propylene oxide by titanium silicate (TS-1) catalyst.[25] Thus, the catalytic activity and recyclability of the new heterogenized O_2 evolution system were investigated together with the *trans–cis* isomerization of the captured *trans*-$[Co(en)_2Cl_2]^+$ species inside the MOF channels. Cowie and Wadi reported that polymer-bound *trans*-$[Co(en)_2Cl(NH_2\text{-polymer})]^{2+}$ derivatives displayed good catalytic activities for O_2 evolution from hydrogen peroxide.[26] The NH_2-polymer derivatives (PMI-TETRAEN and PHpI-TETRAEN) were poly(monomethyl-*co*-dimethyl itaconate) and poly(mono-*n*-heptyl-*co*-di-*n*-heptyl itaconate) functionalized with tetraethylenepentamine. Nevertheless, the recyclability of this polymer-bound system was not fully demonstrated. In this regard, the catalytic activity and recyclability of the heterogenized *trans*-$[Co(en)_2Cl_2]$@InBTB catalytic system were tested for hydrogen peroxide decomposition.

The *trans*-$[Co(en)_2Cl_2]$@InBTB displayed good catalytic activity for the decomposition of hydrogen peroxide to produce oxygen. The catalytic system was stable enough to recycle seven times without significant loss of catalytic activities (Fig. 5a and S3, ESI†). To our surprise, the conversion of hydrogen peroxide was gradually increased upon recycling up to sixth run. In general, the recycling of heterogeneous catalyst tended to show gradual decrease of activity because small amount of catalyst can be lost during recovery. Furthermore, the color of recycled catalyst changed into violet color even after first round of reaction (Fig. 5b). This color change may be attributable to the *trans–cis* isomerization of the captured *trans*-$[Co(en)_2Cl_2]^+$ species. It was speculated that a small portion of the captured *trans*-$[Co(en)_2Cl_2]^+$ kept transforming to *cis*-isomers, either *cis*-$[Co(en)_2Cl(H_2O)]^{2+}$ or *cis*-$[Co(en)_2Cl_2]^+$, during the catalytic reaction. When all captured *trans*-$[Co(en)_2Cl_2]^+$ converted into *cis*-isomers during the recycling experiments, then the reaction rate enhancement was no longer possible. Therefore, the reaction conversion of seventh run was marginally smaller than that of the sixth run. The most widely accepted reaction mechanism for the decomposition of hydrogen peroxide by transition metal active sites suggested potential generation of Co(III)-hydroperoxy species through H–OOH bond activation.[24,27] Based on this proposed reaction mechanism, the above mentioned *cis*-isomers were likely to be more reactive than *trans*-isomer. Also, oxygen bubbles formed right on the surfaces of MOF crystals were able to be observed during the reaction (Fig. 5b). This inferred that the captured *trans*-$[Co(en)_2Cl_2]^+$ species maintained its catalytic activity very well. The concentration of the catalyst was 10 mol% relative to the substrate in the catalytic reaction. Therefore, the turnover number (TON) can be easily calculated from the conversion values. The highest TON for *trans*-$[Co(en)_2Cl_2]$@InBTB during recycling experiment was 6.8 at the 6th recycling. The aforementioned polymer-bound *trans*-$[Co(en)_2Cl(NH_2\text{-polymer})]^{2+}$ derivatives exhibited conversions of ~8% after 9 h with the catalyst concentration of 11.6 mol%.[26] If we compare the conversions after 9 h, *trans*-$[Co(en)_2Cl_2]$@InBTB showed higher activities than *trans*-$[Co(en)_2Cl(NH_2\text{-polymer})]^{2+}$ derivatives as shown in Fig. 5a.

As a control experiment of the color change of *trans*-$[Co(en)_2Cl_2]$@InBTB during the reaction, the reaction condition was emulated in the absence of hydrogen peroxide in water at two different temperatures, 25 and 40 °C. As depicted in Fig. 6a and b, the higher the temperature, the faster the color change. At 25 °C, the green color did not change after 2 h. However, the color of the crystals changed into violet after about 1 h at 40 °C. This implied that the color change was attributable to the *trans–cis* isomerization of the captured *trans*-$[Co(en)_2Cl_2]^+$, because

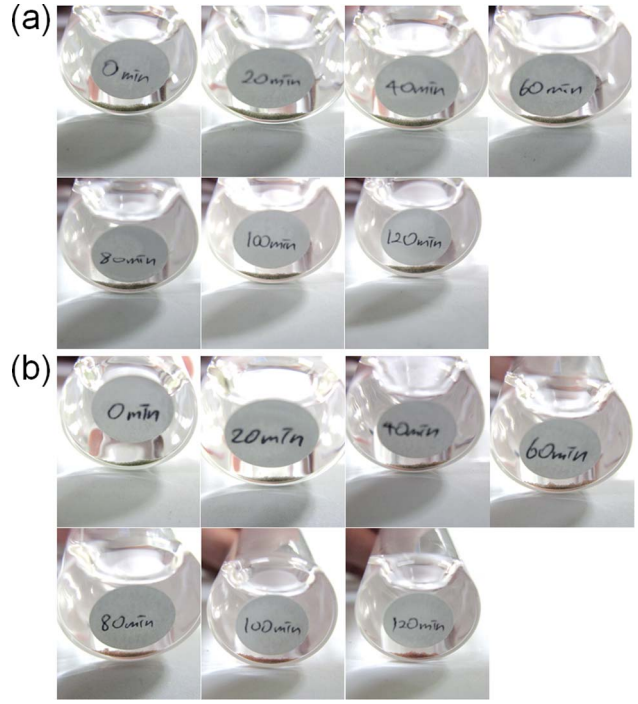

Fig. 6 *Trans*-$[Co(en)_2Cl_2]$@InBTB in deionized water at 25 °C (a) and 40 °C (b).

the isomerization process was temperature dependent.[22] The color change of H_2O_2-treated *trans*-$[Co(en)_2Cl_2]$@InBTB is also clearly discernible as shown in Fig. S4† (ESI).

The Fourier-transform infrared (FT-IR) spectra of the as-prepared InBTB and *trans*-$[Co(en)_2Cl_2]$@InBTB are shown in Fig. 7. The C=O stretching frequency of the DEF solvate in the as-prepared InBTB at 1657 cm^{-1} almost disappeared for *trans*-$[Co(en)_2Cl_2]$@InBTB due to the exchange with *trans*-$[Co(en)_2Cl_2]^+$ ions or ethanol solvent.[28] Contrarily, the deformation signal of $-NH_2$ group in en ligand was newly observed at 1581 cm^{-1} for *trans*-$[Co(en)_2Cl_2]$@InBTB.[21] We also measured the FT-IR spectra of *cis*-$[Co(en)_2Cl_2]Cl$ and *trans*-$[Co(en)_2Cl_2]Cl$ complexes as shown in Fig. S5† (ESI). The stretching frequencies of $-NH_2$ group are slightly different from each other: 1577 cm^{-1} for *cis*-$[Co(en)_2Cl_2]Cl$ and 1594 cm^{-1} for *trans*-$[Co(en)_2Cl_2]Cl$ due to different molecular symmetry. As we proposed earlier, H_2O_2-treated *trans*-$[Co(en)_2Cl_2]$@InBTB showed a signal at 1578 cm^{-1} indicating the possible *trans–cis* isomerization. Thus, the signal observed at 1581 cm^{-1} for *trans*-$[Co(en)_2Cl_2]$@InBTB indicates the formation of *cis*-isomers even in solid state without H_2O_2 treatment. The retrieved *trans*-$[Co(en)_2Cl_2]$@InBTB after catalytic reaction did not show significant IR spectral change compared to *trans*-$[Co(en)_2Cl_2]$@InBTB. Despite the possible isomerization of the captured *trans*-$[Co(en)_2Cl_2]^+$ ion, the FT-IR study indicated that the *trans*-$[Co(en)_2Cl_2]$@InBTB was a highly robust catalytic system for hydrogen peroxide decomposition.

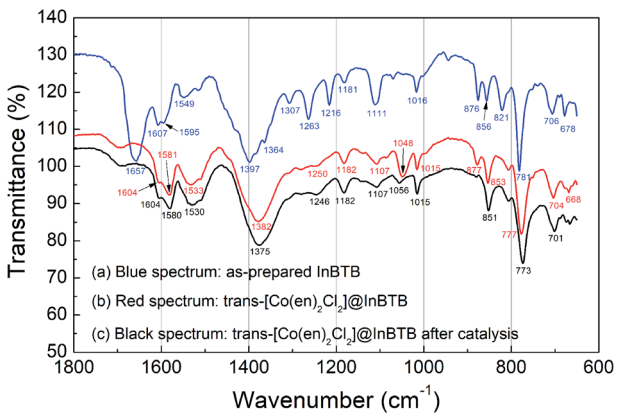

Fig. 7 FT-IR spectra of the as-prepared InBTB (a), *trans*-$[Co(en)_2Cl_2]$@InBTB (b), and the retrieved *trans*-$[Co(en)_2Cl_2]$@InBTB after catalytic reaction (c).

4. Conclusions

The cationic *trans*-$[Co(en)_2Cl_2]^+$ complex was encapsulated into the channels of InBTB through a simple cation-exchange method. The *trans*-$[Co(en)_2Cl_2]$@InBTB was found to be highly recyclable O_2 evolution catalytic system using hydrogen peroxide. The decomposition of hydrogen peroxide could be repeated seven times without significant loss of activity. The activity was gradually enhanced upon recycling possibly because of *trans–cis* isomerization *via* aquation to produce captured *cis*-$[Co(en)_2Cl(H_2O)]^{2+}$ or *cis*-$[Co(en)_2Cl_2]^+$ due to stronger *trans* effect of Cl^- ligand compared to N-donor atom of the en ligand. The latter species were likely to be more active than *trans*-$[Co(en)_2Cl_2]^+$ for the decomposition of hydrogen peroxide. These results were interesting because the mesoscale channels of InBTB behaved as a nanoscale flask for the unprecedented *trans–cis* isomerization of catalytically active transition metal complex in confined spaces. It is believed that employing this basic yet efficient strategy, there will be numerous opportunities to create novel functional MOF systems.

Conflicts of interest

The authors have no conflicts of interest to disclose.

Acknowledgements

This work was supported by grants (2018R1D1A1B07043017 and 2018R1D1A1B07045327) of the Basic Science Research Program through the National Research Foundation (NRF) funded by the Ministry of Education, Science and Technology, Republic of Korea.

Notes and references

1 A. Grigoropoulos, G. F. S. Whitehead, N. Perret, A. P. Katsoulidis, F. M. Chadwick, R. P. Davies, A. Haynes, L. Brammer, A. S. Weller, J. Xiao and M. J. Rosseinsky, *Chem. Sci.*, 2016, **7**, 2037–2050.

2 I.-H. Choi, S. Yoon, S. Huh, S.-J. Kim and Y. Kim, *Chem.–Eur. J.*, 2020, **26**, 14580–14584.
3 S. Yoon, H.-C. Kim, Y. Kim and S. Huh, *Bull. Korean Chem. Soc.*, 2021, **42**, 326–332.
4 E.-Y. Cho, J.-M. Gu, I.-H. Choi, W.-S. Kim, Y.-K. Hwang, S. Huh, S.-J. Kim and Y. Kim, *Cryst. Growth Des.*, 2014, **14**, 5026–5033.
5 J. Yu, Y. Cui, C. Wu, Y. Yang, Z. Wang, M. O'Keeffe, B. Chen and G. Qian, *Angew. Chem., Int. Ed.*, 2012, **51**, 10542–10545.
6 I.-H. Choi, S. B. Yoon, S. Huh, S.-J. Kim and Y. Kim, *Sci. Rep.*, 2018, **8**, 9838.
7 H. K. Chae, D. Y. Siberio-Pérez, J. Kim, Y. Go, M. Eddaoudi, A. J. Matzger, M. O'Keeffe and O. M. Yaghi, *Nature*, 2004, **427**, 523–527.
8 M. Handke, T. Adachi, C. Hu and M. D. Ward, *Angew. Chem., Int. Ed.*, 2017, **56**, 14003–14006.
9 D.-M. Chen, N.-N. Zhang, C.-S. Liu and M. Du, *ACS Appl. Mater. Interfaces*, 2017, **9**, 24671–24677.
10 W. Zhang, R.-Z. Zhang, Y.-Q. Huang and J.-M. Yang, *Cryst. Growth Des.*, 2018, **18**, 7533–7540.
11 R. Grünker, V. Bon, A. Heerwig, N. Klein, P. Müller, U. Stoeck, I. A. Baburin, U. Mueller, I. Senkovska and S. Kaskel, *Chem. - Eur. J.*, 2012, **18**, 13299–13303.
12 G. Lu, S. Li, Z. Guo, O. K. Farha, B. G. Hauser, X. Qi, Y. Wang, X. Wang, S. Han, X. Liu, J. S. DuChene, H. Zhang, Q. Zhang, X. Chen, J. Ma, S. C. J. Loo, W. D. Wei, Y. Yang, J. T. Hupp and F. Huo, *Nat. Chem.*, 2012, **4**, 310–316.
13 H. Liu, L. Chang, C. Bai, L. Chen, R. Luque and Y. Li, *Angew. Chem., Int. Ed.*, 2016, **55**, 5019–5023.
14 B. Gole, U. Sanyal, R. Banerjee and P. S. Mukherjee, *Inorg. Chem.*, 2016, **55**, 2345–2354.
15 M. Mon, M. A. Rivero-Crespo, J. Ferrando-Soria, A. Vidal-Moya, M. Boronat, A. Leyva-Pérez, A. Corma, J. C. Hernández-Garrido, M. López-Haro, J. J. Calvino, G. Ragazzon, A. Credi, D. Armentano and E. Pardo, *Angew. Chem., Int. Ed.*, 2018, **57**, 6186–6191.
16 L. Wang, M. Zheng and Z. Xie, *J. Mater. Chem. B*, 2018, **6**, 707–717.
17 D.-C. Zhong, L.-Q. Liao, J.-H. Deng, Q. Chen, P. Liana and X.-Z. Luo, *Chem. Commun.*, 2014, **50**, 15807–15810.
18 J. C. Bailar, *Inorg. Synth.*, 1946, **2**, 222–225.
19 P. Mialane, C. Mellot-Draznieks, P. Gairola, M. Duguet, Y. Benseghir, O. Oms and A. Dolbecq, *Chem. Soc. Rev.*, 2021, **50**, 6152–6220.
20 Y. Zhou, J. Lu, Y. Zhou and Y. Liu, *Environ. Pollut.*, 2019, **252**, 352–365.
21 J. P. Lanorio and J. G. Lanorio, *J. Lab. Chem. Educ.*, 2018, **6**, 159–163.
22 D. Jacewicz, J. Pranczk, D. Wyrzykowski, K. Żamojć and L. Chmurzyński, *React. Kinet., Mech. Catal.*, 2014, **113**, 321–331.
23 T. E. Khalil, S. M. Soliman, N. A. Khalil, A. El-Faham, S. Foro and A. El-Dissouky, *Appl. Organomet. Chem.*, 2022, **36**, e6565.
24 J. de Laat and H. Gallard, *Environ. Sci. Technol.*, 1999, **33**, 2726–2732.
25 A. Thetford, G. J. Hutchings, S. H. Taylor and D. J. Willock, *Proc. R. Soc. A*, 2011, **467**, 1885–1899.
26 J. M. G. Cowie and N. M. A. Wadi, *Polymer*, 1985, **26**, 1571–1574.
27 J. To, A. A. Sokol, S. A. French and C. R. A. Catlow, *J. Phys. Chem. C*, 2008, **112**, 7173–7185.
28 I.-H. Choi, Y. Kim, D. N. Lee and S. Huh, *Polyhedron*, 2016, **105**, 96–103.